Journal of Alloys and Compounds 609 (2014) 68–72

Contents lists available at ScienceDirect

Journal of Alloys and Compounds

journal homepage: www.elsevier.com/locate/jalcom

Synthesis, photoluminescence and optical constants evaluations of ultralong CdO nanowires prepared by vapor transport method

S.H. Mohamed *, N.M.A. Hadia, A.K. Diab, A.M. Abdel Hakeem

Physics Department, Faculty of Science, Sohag University, 82524 Sohag, Egypt

ARTICLE INFO

Article history:
Received 21 February 2014
Received in revised form 8 April 2014
Accepted 9 April 2014
Available online 24 April 2014

Keywords:
CdO NWs
Vapor transport
FT-IR
SEM
Ellipsometer
Photoluminescence

ABSTRACT

Ultralong CdO nanowires (NWs) were synthesized on Au coated Si and quartz substrates by using vapor transport method. The synthesis temperature was chosen via thermal gravimetry analysis (TGA) and it was 1150 °C. The formation of CdO was confirmed by energy dispersive analysis of X-ray (EDAX) and Fourier transform infrared (FT-IR) spectroscopy analysis. The CdO nanowires was found to grow via a vapor–solid growth mechanism. The diameters of the nanowires were in the range 30–90 nm and the lengths were greater than 30 μm. The optical constants, the thickness and the surface roughness of the prepared CdO NWs films were determined by spectroscopic ellipsometry measurements. A two layers model was used to fit the calculated data to the experimental ellipsometric spectra. The obtained optical constants were compared with those obtained by other preparation methods. The optical band gap was found to be 2.41 eV. An emission peak at ~550 nm was recorded, which should corresponds to the near band-edge emission of CdO.

1. Introduction

Low dimensional (0D and 1D) nanoscale semiconducting metal oxide materials have attracted much attention because they have new functional properties and numerous applications [1–3]. The synthesis of metal oxide nanowires with uniform shape and diameter has special interest because they have large surface area and provide superior electrical conductivity when compared to other morphologies [4,5]. Also, the mixed nanostructures such as nanowires mixed with nanoparticles, nanowires mixed with nanosheets and dendrites nanowires have also important applications [6–8].

Low dimensional cadmium oxide (CdO), as an important n-type semiconductor metal oxide, has also widely investigated owing to its potential applications in optical fields, photovoltaic cells and transparent electrodes [9–11]. So far, various 1D CdO nanostructures have been prepared through different synthetic routes. For example, CdO nanowires, nanoneedles, nanobelts and nanorods have been obtained by chemical bath deposition [11], solvothermal method [12] and vapor phase transport [13,14]. However, the work done for 1D CdO nanostructures by vapor phase transport is still very few. Therefore we report the synthesis of uniform and ultralong CdO nanowires by a simple vapor transport method. The crystal structure, the chemical composition, photoluminescence and the optical constants are analyzed.

2. Experimental

The CdO nanowires were grown using evaporation–condensation method with VLS growth technique. The synthesis processes of CdO were carried out in a controllable horizontal tube furnace with an alumina tube (inner diameter of 44 mm and length of 90 cm). The synthesis was carried out on Au coated (~5–10 nm) Si (100) wafers and quartz substrates (cut into 1 cm × 1 cm and ultrasonically cleaned). The Au coating of the substrates were done using AC Ion sputtering device (JFC-1100E). The CdO nanostructures were prepared using CdO powder, (Aldrich chemicals; 99.999%). The CdO was placed in an alumina boat positioned at the center of the heating zone of the furnace. The Au coated Si substrates were placed downstream where they were covering a distance of 7–15 cm from the alumina boat. A mixture of flowing Ar with 300 sccm (standard cubic centimeter per minute) and O_2 with 20 sccm was introduced into the alumina tube. Concurrently the temperature was raised 10 °C/min up to 1150 °C and kept for 30–60 min. After that, the furnace was cooled down to room temperature.

The thermal gravimetry analysis (TGA) was employed to determine the synthesis temperature for the CdO precursor using Schemadzu DTG-60AH Thermo-gravimetric Analyzer. A sample (mass app. 2.993 mg) was heated in a standard platinum pan. The measurements were carried out in air atmosphere. The heating rate was 20 °C/min and started from RT to 1400 °C.

The surface morphology and crystal structure of the synthesized nanostructures were characterized by scanning electron microscope (SEM) type JOEL model JSM-6380 LA (Japan) and X-ray diffraction (XRD) using Shimadzu Diffractometer XRD 6000, Japan, which utilizing Cu Kα1 radiation (λ = 1.54056 Å), respectively. The chemical composition of the synthesized nanostructures was analyzed using energy dispersive analysis of X-ray (EDAX) unit attached with the SEM. Transmission electron microscopy (TEM) images were obtained with a 2000 EX II microscope (JEOL,

* Corresponding author. Tel.: +20 966 0558744839; fax: +20 966 3800911.
E-mail address: abo_95@yahoo.com (S.H. Mohamed).

http://dx.doi.org/10.1016/j.jallcom.2014.04.065
0925-8388/

Japan) at an acceleration voltage of 200 kV. For TEM observation, the synthesized products were ultrasonically dispersed in ethanol and a drop of the suspension was placed on a Cu grid coated with carbon film.

Powder of CdO was scratched easily out of the Au coated Si substrate, grounded and used for Fourier transformation infrared (FT-IR) analysis. The CdO powder was mixed with KBr for FT-IR measurements. The FT-IR measurements were carried out using a Fourier transformation infrared spectrophotometer (IRPrestige-21, SHIMADZU) in the wavenumber range 400–4000 cm^{-1} with 3.85 cm^{-1} resolution and at room temperature (RT).

The spectroscopic ellipsometry (SE) data for CdO nanostructured films were acquired using a PHE-102 variable angle spectroscopic ellipsometer (Angstrom Advanced Inc.) in the wavelength range 350–1100 nm (energy range 3.54–1.13 eV). The data were acquired at three deferent angles of incidence of 60°, 65° and 70°. The instrument measures the complex ratio of the Fresnel reflection coefficients for p- and s-polarized light and reports the ratio in terms of the ellipsometric parameters Ψ and Δ defined by the following equation:

$$F = \tan(\Psi)\exp(i\Delta) = \frac{\tilde{r}_p}{\tilde{r}_s} \quad (1)$$

where $\tilde{r}_p$ and $\tilde{r}_s$ are the amplitude reflection coefficient for light polarized in the p- and s-plane of incidence, respectively. The data obtained from the ellipsometer were accurately modeled using the PHE-102 software package. Ellipsometric data Ψ and Δ for variable wavelengths were fitted in the optical model.

The spectral transmittance (T) and reflectance (R) of the synthesized nanostructures, on Au coated quartz substrates, were measured by a JASKO V-570 spectrophotometer in the wavelength range 200–2500 nm. The room temperature photoluminescence (PL) spectrum of the products was measured using Edinburgh Instruments FLS920 steady-state fluorescence spectrometer (UK) with Xe lamp as the excitation light source (with a wavelength of 350 nm).

3. Results and discussion

3.1. Structural, morphological, compositional and thermal examinations

The choice of the synthesis temperature was based on the thermal stability of the CdO precursor. Fig. 1a shows the TGA thermogram of the CdO precursor. It can be seen that the CdO precursor is almost stable up to 1050 °C, above which a large weight loss is observed. The weight loss becomes much sharper at 1150 °C, which has been chosen for the preparation of CdO nanowires. The negative TGA values observed between 1300 °C and 1400 °C may be ascribed to the removal of water adsorbed at the crucible.

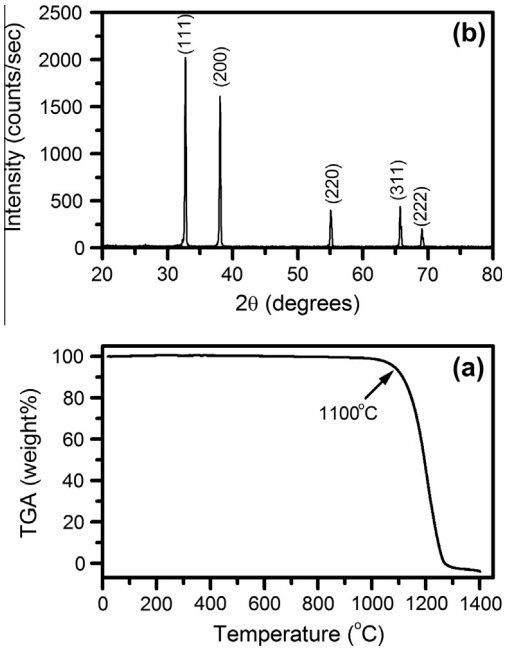

Fig. 1. TGA thermogram of the CdO precursor (a) and XRD pattern of CdO NWs (b).

Fig. 1b shows the XRD pattern of CdO nanostructure. The existence of sharp peaks in this figure indicates that the CdO nanostructure has a polycrystalline nature with high degree of crystallinity. All the diffraction peaks can be indexed to CdO with cubic structure (JCPDS file no. 78-0653). The pattern also confirms that there are no Cd characteristics peaks. The lattice parameter (a) was calculated from the equation:

$$a = d\sqrt{h^2 + k^2 + l^2} \quad (2)$$

where d is the spacing between adjacent (hkl) planes. The lattice parameter is a = 4.725 Å. The mean grain size, calculated from the Scherrer formula [15], is 49 nm. Harris analysis was performed to investigate the preferential orientation of the crystallographic planes in the CdO nanostructure. The texture coefficient $P(h_i k_i l_i)$, a preferential orientation indicator of the $(h_i k_i l_i)$ plane, is given by the following equation [16]:

$$P(h_i k_i l_i) = \left(\frac{I(h_i k_i l_i)}{I_r(h_i k_i l_i)}\right)\left(\frac{1}{m}\sum_{i=1}^{m}\frac{I(h_i k_i l_i)}{I_r(h_i k_i l_i)}\right)^{-1} \quad (3)$$

where $I(h_i k_i l_i)$ is the diffraction intensity of the $(h_i k_i l_i)$ plane of the sample under investigation, $I_r(h_i k_i l_i)$ is the intensity of the $(h_i k_i l_i)$ plane of a random powder sample and m is the number of diffraction peaks. Eq. (3) shows that $P(h_i k_i l_i)$ of each crystallographic plane

Table 1
X-ray diffraction intensities and preferred orientation factors of CdO nanowires.

(hkl)	I	I_r[a]	P_{hkl}
(111)	2004	999	1.72
(200)	1596	857	1.60
(220)	383	459	0.72
(311)	416	291	1.23
(222)	194	125	1.33

[a] From JCPDS, International Centre for Diffraction Data, 1996.

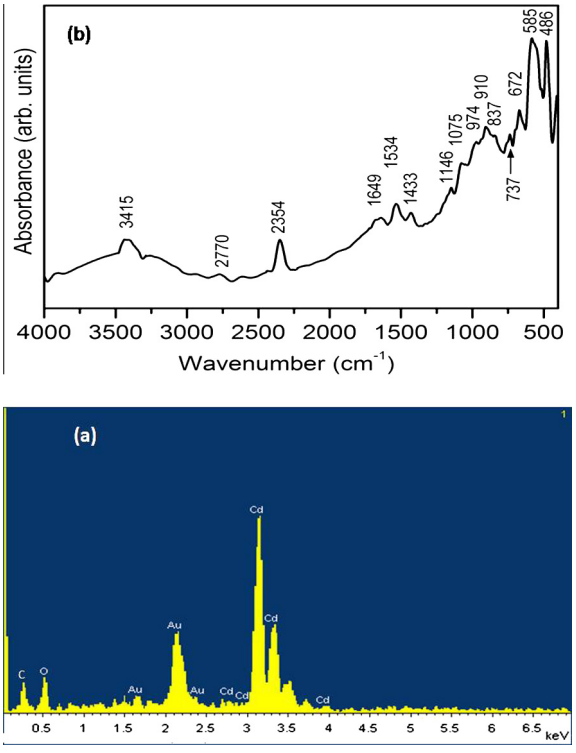

Fig. 2. EDAX spectrum (a) and FT-IR spectrum (b) for CdO NWs.

is unity for a randomly distributed powder sample, whereas is larger than unity if ($h_i k_i l_i$) plane is preferentially oriented. The Harris analysis results are summarized in Table 1. The texture coefficient value of the index (1 1 1) plane is the highest indicating that is more preferentially oriented.

The atomic percentages of Cd and O were evaluated by EDAX (Fig. 2a), on Si substrates, and are found to be 50.81 and 49.19 at.%, respectively. The results indicates the formation of the CdO. The FT-IR spectrum for the prepared CdO nanowires is shown in Fig. 2b. The strong absorption band at 3415 cm^{-1} is attributed to stretching vibrations of surface hydroxyl group (O–H). The band at 2770 cm^{-1} is to the symmetric stretching vibrations of C–H group. The strong band at 2354 cm^{-1} and the bands at 1649, 1534, 1433, 1146 and 1075 cm^{-1} could be ascribed to v_s(C–O) and v_{as}(C–O) vibrations of atmospheric CO_2, which results from the preparation and processing of FT-IR samples in the ambient atmosphere [17]. The typical absorption bands from 974 cm^{-1} to 413 cm^{-1} are characteristics of the metallic bonds and are ascribed to Cd–OH and the Cd–O groups [18,19].

Fig. 3a and b shows low and high magnifications of SEM image of the CdO nanowires grown on a silicon substrate. There is a dense growth of uniform and long nanowires. Most of the nanowires have lengths greater than 30 μm. The diameters of these nanowires range mostly between 30 and 90 nm. To further analyze the crystal structure of CdO nanowires, TEM characterization of the nanowires was conducted. Fig. 3c–d represent TEM images. Although the nanowires have different diameters, the single nanowire has a uniform diameter with smooth surface. The examination of a single CdO nanowire (Fig. 3d) shows that there is no clear evidence for particles or dotes can be found at the tips of these nanowires. This suggested that the nanowires are formed via vapor–solid (VS) growth mechanism. It is worth mentioning that length and diameters of the nanowires depend on different preparation factors as well as the preparation methods [13,20].

3.2. Optical constants

SE data were analyzed by a multilayer model consisting of the ambient, a surface overlayer, the main CdO layer and the Si(100) substrate. The optical response of the surface overlayer was modeled within a Bruggeman effective medium approximation (BEMA). The main CdO layer was described by Lorenz oscillator model [21]. The optical constants of Si obtained by Herzinger et al. [22] were used for the Si(100) substrate. An example for the quality of the fits results of the experimental and fitted ellipsometry data is shown in Fig. 4. The thicknesses of the surface overlayer and the main CdO layer are 6.4 nm and 67.2 nm.

The refractive index (n) and extinction coefficient (k) dependences on wavelength are illustrated in Fig. 5. The refractive index decreases with increasing wavelength up to 545 nm, above which the refractive index increases continually with increasing wavelength. This behavior is similar to that observed by Ziabari et al. [23] for un-doped and Al doped cadmium oxide thin films deposited on glass substrates by sol–gel dip coating method. However the refractive index values are lower than their obtained values. The k values decrease with increasing wavelength and became

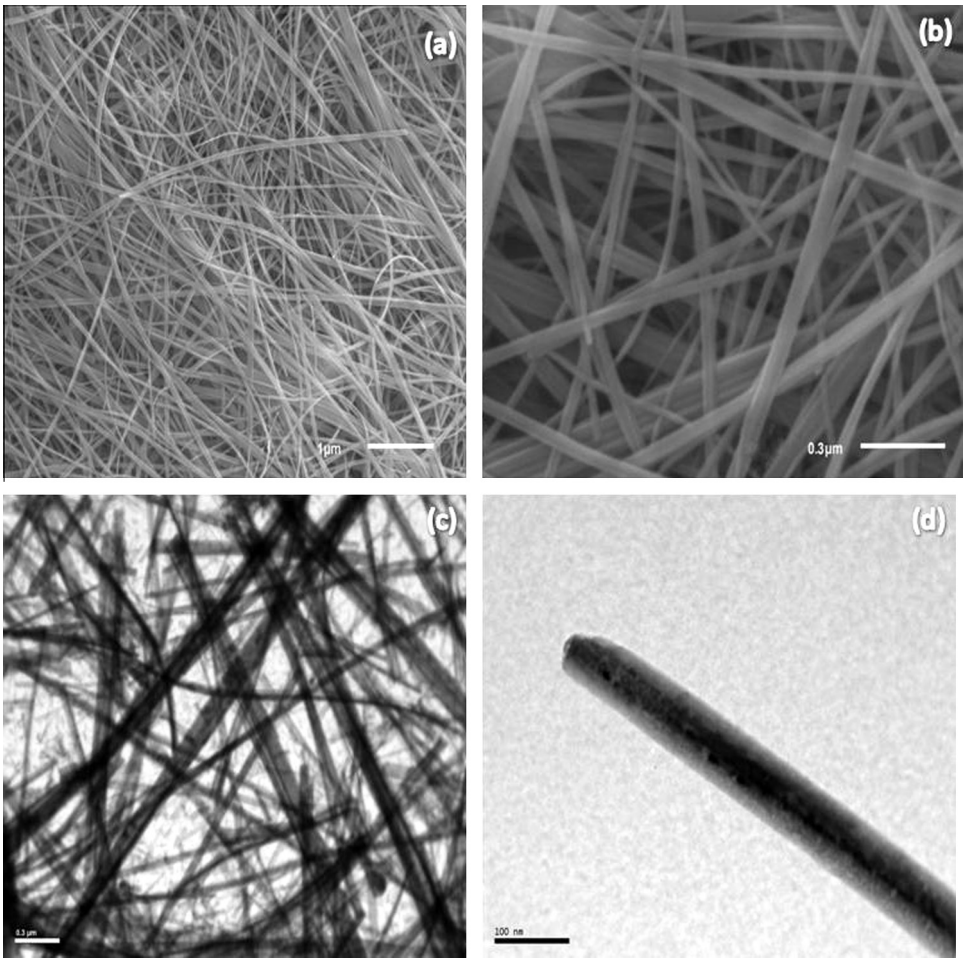

Fig. 3. SEM image (a and b) of CdO NWs with low (0.3 μm) and high (1 μm) magnifications. TEM images (c and d) of CdO NWs with low (100 nm) and high (0.3 μm) magnifications.

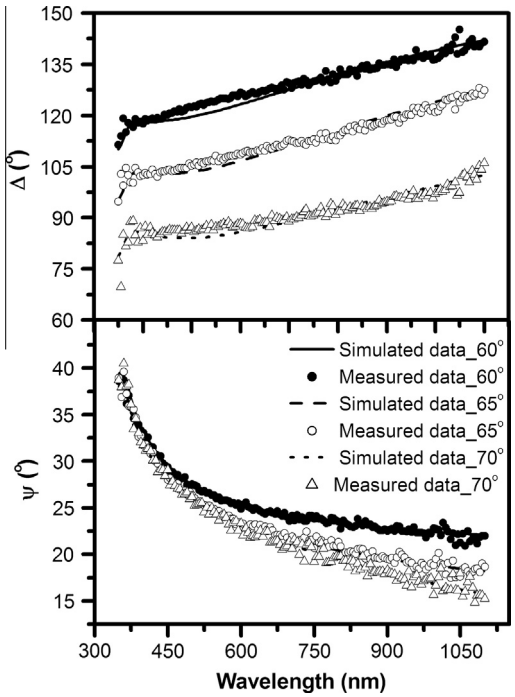

Fig. 4. Measured and calculated Ψ and Δ spectra at 60°, 65° and 70° angles of incidence for CdO NWs film.

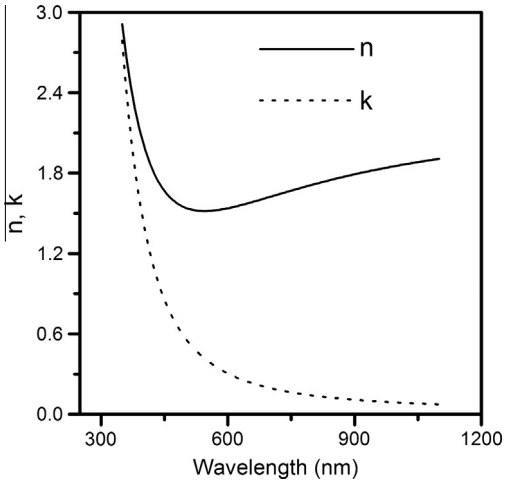

Fig. 5. The refractive index and extinction coefficient of CdO NWs film.

much closer to zero at higher wavelengths. It is known that the k values depend on the absorption by atoms, the surface roughness, the polycrystalline grain size and the defects in the film [24].

The optical transmittance (T) and reflectance (R) spectra of CdO sample prepared on quartz substrate are presented in Fig. 6a. As seen in Fig. 6a, the optical transmittance decreases gradually up to 900 nm below which the transmittance decreases strongly with the decrease in wavelength. The sharp decrease in transmittance at the wavelength $\lambda < 900$ nm is due to the onset of interband transitions at the fundamental edge. The reflectance remains almost constant up to 550 nm below which the reflectance increases strongly with the decrease in wavelength.

The optical absorption in the UV region is dominated by the optical band gap of the semiconductor. The optical band gap (E_g) of a semiconductor is related to the optical absorption coefficient (α) and the incident photon energy ($h\nu$) by [25]

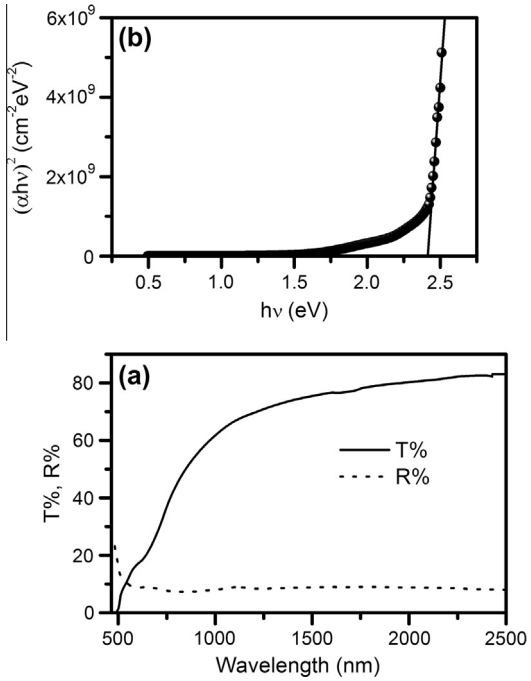

Fig. 6. Optical transmittance (T) and reflectance (R) spectra for CdO NWs film (a). Plot of $(\alpha h\nu)^2$ versus $h\nu$ for CdO NWs film (b).

$$(\alpha h\nu) = \beta(h\nu - E_g)^{\eta} \quad (4)$$

where η depends on the kind of optical transition that prevails. Specially, η is 1/2 and 2 when the transition is directly and indirectly allowed, respectively. The CdO sample is known to be a semiconductor with a directly allowed transition [26]. The optical band gap is obtained fom $(\alpha h\nu)^2$ versus $h\nu$ plot and extrapolating the linear portion of the curve to $(\alpha h\nu)^2 = 0$ (Fig. 6b). The optical band gap of the CdO NWs sample is found to be 2.41 eV. This is in good agreement with the previously reported values of 2.4 eV and 2.42 eV [27,28].

3.3. Photoluminescence (PL)

Fig. 7 shows the photoluminescence spectrum of CdO NWs that is measured at room temperature using the excitation wavelength of 350 nm. An emission peak at ~550 nm is recorded, which should corresponds to the near band-edge emission of CdO. The photoluminescence spectra of CdO have been reported by many research-

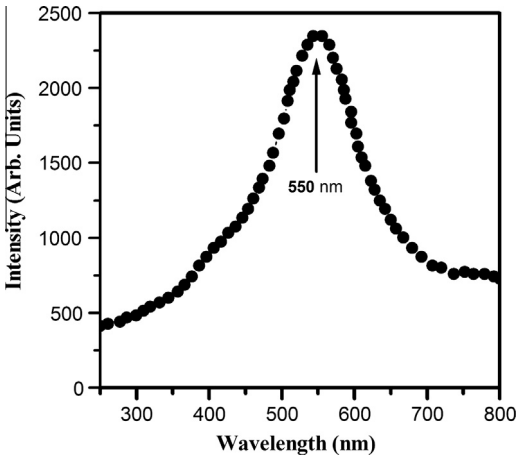

Fig. 7. Photoluminescence spectrum of CdO NWs.

ers [29–32] which suggest that the band at 484 nm arises from the transition between the conduction and valence bands. The band at 550 nm is due to near band-gap radiative recombination [33]. The suggested mechanism of the green emission (490–570 nm) is mainly due to the concentration of free electrons, and the existence of various point defects identified as V_o due to the heat treatments and or oxidation associated with the process which helps form the recombination centers [34]. With such a strong emission peak at ~550 nm, the CdO NWs can be utilized in the industry of high quality monochromatic laser [35].

4. Conclusions

Ultralong CdO NWs were grown on Si and quartz substrates via vapor transport method. XRD analysis revealed that the product is a single crystalline phase of cubic CdO. The nanowires were synthesized by VS growth mechanism. The NWs have smooth surfaces, diameters in the range of 30–90 nm and lengths greater than 30 μm. The thickness and optical constants were accurately determined from the SE which may prove useful in the design of nano-optoelectronic devices. The strong emission peak at ~550 nm indicates that the CdO NWs can be utilized in the industry of high quality monochromatic laser.

References

[1] M. Zirak, O. Akhavan, O. Moradlou, Y.T. Nien, A.Z. Moshfegh, J. Alloys Comp. 590 (2014) 507–513.
[2] E. Comini, C. Baratto, I. Concina, G. Faglia, M. Falasconi, M. Ferroni, V. Galstyan, E. Gobbi, A. Ponzoni, A. Vomiero, D. Zappa, V. Sberveglieri, G. Sberveglieri, Sens. Actuator B 179 (2013) 3–20.
[3] B. Kulyk, V. Kapustianyk, V. Tsybulskyy, O. Krupka, B. Sahraoui, J. Alloys Comp. 502 (2010) 24–27.
[4] S. Wang, Z.-X. Lin, W.-H. Wang, C.L. Kuo, K.C. Hwang, C.-C. Hong, Sens. Actuator B 194 (2014) 1–9.
[5] P. Afzali, Y. Abdi, E. Arzi, Sens. Actuator B 195 (2014) 92–97.
[6] S.H. Mohamed, J. Alloys Comp. 510 (2012) 119–124.
[7] N.M.A. Hadia, H.A. Mohamed, J. Alloys Comp. 547 (2013) 63–67.
[8] K. Dai, L. Lu, C. Liang, J. Dai, Q. Liu, Y. Zhang, G. Zhu, Z. Liua, Electrochim. Acta 116 (2014) 111–117.
[9] K. Kaviyarasu, E. Manikandan, P. Paulraj, S.B. Mohamed, J. Kennedy, J. Alloys Comp. 593 (2014) 67–70.
[10] A. Yousef, N.A.M. Barakat, S.S. Al-Deyab, R. Nirmala, B. Pant, H.Y. Kim, Colloid. Surf. A: Physicochem. Eng. Aspects 401 (2012) 8–16.
[11] A.S. Kamblea, R.C. Pawara, J.Y. Patil b, S.S. Suryavanshib, P.S. Patil, J. Alloys Comp. 509 (2011) 1035–1039.
[12] K. Kaviyarasu, E. Manikandan, P. Paulraj, S.B. Mohamed, J. Kennedy, J. Alloys Comp. 593 (2014) 67–70.
[13] T.-J. Kuo, M.H. Huang, J. Phys. Chem. B 110 (2006) 13717–13721.
[14] T. Terasako, T. Fujiwara, Y. Nakata, M. Yagi, S. Shirakata, Thin Solid Films 528 (2013) 237–241.
[15] B.D. Cullity, Elements of X-ray Diffraction, second ed., Addison-Wesley, Reading, MA, 1979. p. 102.
[16] C.S. Barrett, T.B. Massalski, Structures of Metals, Pergamon, Oxford, 1980. p. 204.
[17] Z. Guo, M. Li, J. Liu, Nanotechnology 19 (2008) 245611–245618.
[18] B. Malecka, A. Lacz, Thermochim. Acta 479 (2008) 12–16.
[19] A. Tadjarodi, M. Imani, Mater. Lett. 65 (2011) 1025–1027.
[20] G. Zhu, Y. Zhou, S. Wang, R. Yang, Y. Ding, X. Wang, Y. Bando, Z. Wang, Nanotechnology 23 (2012) 055604–55606.
[21] S.H. Mohamed, Philos. Magn. 91 (2011) 3598–3612.
[22] C.M. Herzinger, B. Johs, W.A. McGahan, J.A. Woollam, W. Paulson, J. Appl. Phys. 83 (1998) 3323–3336.
[23] A.A. Ziabari, F.E. Ghodsi, G. Kiriakidis, Surf. Coat. Technol. 213 (2012) 15–20.
[24] S.H. Mohamed, M. El-Hagary, Mater. Chem. Phys. 143 (2013) 178–183.
[25] N.F. Mott, E.A. Davis, Electronic processes in noncrystalline materials, in: W. Marshall, D.H. Wilkinson (Eds.), Clarendon Press, Oxford, 1979, pp. 272–293.
[26] D.J. Seo, J. Korean Phys. Soc. 45 (2004) 1575–1579.
[27] S. Weng, M. Concivera, J. Electrochem. Soc. 139 (1992) 3220–3224.
[28] C. Sravani, K.T.R. Reddy, P.J. Reddy, Semicon. Sci. Technol. 6 (1991) 1036–1038.
[29] X. Wu, R. Wang, B. Zou, L. Wang, S. Liu, J. Xu, J. Mater. Res. 13 (1998) 604–609.
[30] M. Benhaliliba, C.E. Benouis, A. Tiburcio-Silver, F. Yakuphanoglu, A. Avila-Garcia, A. Tavira, R.R. Trujillo, Z. Mouffak, J. Lumin. 132 (2012) 2653–2658.
[31] N.A.M. Barakat, S. Al-Deyab, H.Y. Kim, Mater. Lett. 66 (2012) 225–228.
[32] Haiyan Li, Yanxue Chen, Jun Jiao, Nanotechnology 20 (2009) 225601–225606.
[33] M. Ghosh, C.N.R. Rao, Chem. Phys. Lett. 393 (2004) 493–497.
[34] R. Dingle, Phys. Rev. Lett. 23 (1969) 579–581.
[35] Z. Yang, W. Zhong, Y. Yin, X. Du, Y. Deng, C. Au, Y. Du, Nanoscale Res. Lett. 5 (2010) 961–965.